https://doi.org/10.5194/hess-2019-686
Preprint. Discussion started: 14 January 2020

Hydrology and Earth System Sciences
Discussions

Do streamwater solute concentrations reflect when connectivity occurs in a small pre-alpine headwater catchment?

Leonie Kiewiet[1], Ilja van Meerveld[1], Manfred Stähli[2], Jan Seibert[1,3]
[1]Department of Geography, University of Zürich, Zürich, Switzerland
[2]Swiss Federal Research Institute WSL, Birmensdorf, Switzerland
[3]Department of Aquatic Sciences and Assessment, Swedish University of Agricultural Sciences, Uppsala, Sweden

Correspondence to: Leonie Kiewiet (leonie.kiewiet@geo.uzh.ch)

Abstract. Expansion of the hydrologically connected area during rainfall events causes previously disconnected areas to contribute to streamflow. If these contributing areas have a different hydrochemical composition than the permanently connected areas, this may cause a change in streamwater chemistry that can not be described by simple mixing of rainfall and baseflow. Changes in stormflow composition are therefore sometimes used to identify when transiently disconnected areas (or water sources) contribute to stormflow. We identified the dominant sources of streamflow for four rainfall events in a steep 20-ha pre-alpine headwater catchment in Switzerland to investigate the temporal changes in connectivity. First, we compared the isotopic and chemical composition of stormflow at the catchment outlet to the composition of rainfall, groundwater, and soil water. Three-component end-member mixing analyses indicated that groundwater dominated stormflow for three of the four events, and that soil water fractions were minimal for two events. Then, we tested whether conservative mixing of rainfall and baseflow could describe the chemical composition of stormflow. To this end, we estimated the concentrations of different solutes in stormflow based on the mixing fractions derived from a conservative tracer (δ^2H) and the concentration of the solutes in baseflow and rainfall. Then, we compared these estimated concentrations to the measured concentrations. We found that the estimated concentrations differed from the measured stormflow concentrations for many solutes and samples. The deviations increased gradually with streamflow for some solutes (e.g., iron and copper), suggesting increased hydrologic connectivity. However, the large variability in soil and groundwater composition compared to the changes in stormflow inhibited the determination of the contributions from the different sources. Our findings show that solute concentrations can be helpful for investigating hydrologic connectivity, and that it is important to quantify the variability in the composition of different source areas.

1 Introduction

During dry periods only a small part of the catchment is connected to the stream, but the connected area can expand dramatically during rainfall or snowmelt events (Stieglitz et al., 2003; Bracken and Croke, 2007; Jencso and McGlynn, 2011; van Meerveld et al., 2015). For example, Ladouche et al. (2001) showed for the Strengbach catchment (France) that the upper layers of saturated areas (2% of surface area, mainly in the lower part of the catchment) contributed up to 30% of the discharge during the initial stages of a rainfall event, whereas upslope and downslope layers contributed equally to flow during the final stage of the event. Oswald et al. (2011) showed for a catchment in the Experimental lakes region in northwestern Ontario, Canada, that a large part of the catchment area was hydrologically disconnected from the stream during most events, and that there was a threshold after which a larger area contributed to streamflow. Connection of upslope areas does not only lead to large changes in discharge (Lehmann et al., 2007; Detty and Mcguire, 2010) but can also cause major changes in stream water composition (e.g., Devito and Hill, 1997; Stieglitz et al., 2003; Ocampo et al., 2006).

Direct observation of hydrologic connectivity is challenging because it is difficult to quantify subsurface processes (Hopp and McDonnell, 2009; Blume and van Meerveld, 2015). Hillslope-stream connectivity can be inferred from hillslope-based measurements or stream-based measurements (Blume and van Meerveld, 2015). Stream-based interpretations of connectivity

https://doi.org/10.5194/hess-2019-686
Preprint. Discussion started: 14 January 2020

are usually based on changes in stream chemistry during events. Few studies have compared the results from stream-based and hillslope-based inferences of connectivity. For instance, Burns et al (1998) showed that hillslope contributions to streamflow based on end-member mixing analysis were similar to the subsurface flow measurements for a trenched hillslope. In many studies, conservative tracers (e.g. stable water isotopes or non-reactive elements) are selected to identify the origin of streamflow, using methods such as hydrograph separation (Buttle, 1994) or end-member mixing analyses (EMMA; Hooper et al., 1990; Christophersen and Hooper, 1992). Von Freyberg et al. (2014) used the composition of stormflow during 31 rainfall events and the composition of shallow groundwater to show that streamflow in the Rietholzbach catchment gradually shifted from a riparian-zone composition to a more hillslope-dominated composition as the lower parts of the hillslopes became hydrologically connected to the river network. McGlynn and McDonnell (2003) used concentrations of silica and isotope data to show for a 2.6-ha sub-catchment of the Maimai catchment in New Zealand that the fraction of water from the hillslopes was larger for an event with higher wetness conditions than for an event with drier initial conditions, and that hillslope contributions were larger on the falling limb of the hydrograph.

Non-conservative solute concentrations can also provide useful information on hydrological connectivity and flow pathways because they can aid the identification of different source areas (Barthold et al., 2011). For instance, Soulsby et al. (2008) used Gran alkalinity as a tracer for groundwater and soil water contributions in the Feshie catchment in Schotland. The concentrations of specific elements can also be indicative for differences in redox conditions (e.g., sulfate, iron, manganese), bedrock-contact time (e.g., calcium, magnesium, sodium, barium) or vegetation (e.g., nitrogen, phosphorus, potassium) (Kaushal et al., 2018). Solute concentrations in stream water might be relatively constant (chemostatic), decrease (dilution) or increase (mobilization) in response to rainfall, depending on the source areas to streamflow and their respective concentrations, as well as reactive transport processes (Godsey et al., 2009; Seibert et al., 2009). Godsey et al. (2009) found that concentrations of typical weathering products (calcium, magnesium, silica and sodium) were nearly chemostatic for 59 geochemically diverse US catchments, indicating that there should be a (constant) source of these solutes. This suggests that the areas that connect during rainfall events have similar concentrations of these solutes as the permanently contributing areas or higher concentrations to compensate the dilution caused by the rainfall, or that reactions are fast enough to maintain similar concentrations during the event. The timing of the onset of contributions from different source areas also affects the solute concentrations (Abbott et al., 2018). Several studies have shown that the relation between concentration and stormflow is hysteretic at the event time scale (e.g., Evans and Davies, 1998; Hornberger et al., 2001). Zuecco et al. (2019) showed that subsurface connectivity increased later than streamflow (anti-clockwise hysteresis) for two sub-catchments of the Studibach catchment (Switzerland), suggesting that hillslope runoff may not be a dominant runoff source at the beginning of rainfall events for these small catchments. This can cause a hysteretic relation between solute concentration and streamflow if hillslope and riparian zone water have a different composition. Changes in solute concentrations might also depend on the size of the catchment (Brown et al., 1999) and mixing that might occur on the way from the source areas to the outlet. For instance, hillslope runoff may bypass the riparian zone through focused locations along the stream channel or via preferential flow pathways (Allaire et al., 2015), and mix with other hillslope sources (Seibert et al., 2009) and riparian groundwater (McGlynn and McDonnell, 2003) on its way to the stream.

It has been suggested that the discrepancy between hydrograph separation results for conservative and non-conservative tracers highlights when and where streamwater is not the result of conservative mixing between end-members, such as baseflow and precipitation (Kirchner, 2003). Instead, it might reflect mixing from different ‘old’ water sources in the catchment that have different concentrations. Therefore, this discrepancy may provide information on when hillslope-stream connectivity is established. Alternatively, these differences might be (partly) due to reactive processes that mobilize (or immobilize) solutes at the event-time scale (Godsey et al., 2009). As such, focusing on solute responses in stormflow, and the difference between

https://doi.org/10.5194/hess-2019-686
Preprint. Discussion started: 14 January 2020

Hydrology and Earth System Sciences
Discussions

conservative and non-conservative tracers, might allow us to identify the extent of these reactive transport processes, and contributions from 'old' water sources that do not contribute to baseflow.

In this study, we combined spatially distributed soil- and groundwater sampling with event-based streamwater sampling in the pre-alpine Studibach catchment to address the following research questions:

1. How variable is streamwater chemistry during events compared to the spatial variability in soil and groundwater chemistry?
2. What are the dominant sources of streamflow during small to intermediately sized rainfall events?
3. Does conservative mixing of baseflow and rainfall explain the changes in the solute concentrations or must other sources contribute to stormflow as well? If other sources contribute to stormflow, what are their characteristics and when do they contribute to flow?

2. Study catchment

We conducted this study in the 20-ha pre-alpine Studibach catchment, a headwater catchment of the Zwäckentobel, located in the Alptal, Switzerland. The elevation ranges from 1,270 to 1,650 m above sea level. The mean annual precipitation of about 2,300 mm y^{-1} is relatively evenly distributed throughout the year (Feyen et al., 1999), and about one-third falls as snow (Stähli and Gustafsson, 2006). Streamflow and groundwater levels respond quickly to rainfall (Fischer et al., 2015; Rinderer et al., 2015). The median groundwater level response time is generally less than 30 minutes (Rinderer et al., 2014) and for many events only 3-mm of cumulative rainfall already causes an increase in the groundwater level for a large part of the catchment (Rinderer et al. 2015). Generally, the groundwater level peak preceeds peak discharge in the Studibach at half of the sites, but only by 15 or 20 minutes (Rinderer et al., 2015). Water levels in flatter locations and topographic depressions rise nearly instantaneously, which suggests that they can contribute to streamflow during the early stages of the rainfall event. Event water fractions in stormflow are generally low (Kiewiet et al., in review; von Freyberg et al., 2018), except for events exceeding 50-mm of rainfall (Fischer et al., 2017). The catchment is steep (average slope: 35°) and characterized by a step-wise topography of flatter areas and steep slopes due to soil creep and landslides. About half of the catchment is covered by an open coniferous forest (Hagedorn et al., 2000), a third is characterized as a moor landscape or wet grassland, and the remaining areas are alpine meadows.

Soil depth is weakly correlated to slope (van Meerveld et al., 2018) but generally shallow (0.5 m at ridge sites to ~2.5 m in depressions). The gleysols are underlain by three different types of Flysch bedrock, which is a reworked carbonate rock consisting of deep-water and turbidite deposits. The carbonate-rich bedrock results in high solute concentrations with a calcium-bicarbonate signature, although some sites have high sulfate and magnesium concentrations (Kiewiet et al., 2019).

The Studibach can be subdivided into four different landscape elements with a distinct groundwater composition (Kiewiet et al., 2019 and Fig. 1):

1. Riparian zone, flatter areas and topographic hollows with above average concentrations of iron and manganese. These areas are from here on referred to as 'riparian';
2. Hillslopes and steeper areas, characterized by above average concentrations of copper, zinc and lead;
3. Areas with above average concentrations of weathering-derived solutes, such as strontium, indicative of longer (and deeper) flow pathways, which are from here on referred to as deep wells;
4. Areas located in a specific part of the catchment that are characterized by high magnesium and sulfate concentrations.

https://doi.org/10.5194/hess-2019-686
Preprint. Discussion started: 14 January 2020

3. Methods

3.1 Sample collection

We analysed the streamflow and stream chemistry for four events (I-IV; Table 1) in fall 2016 and 2017. Stream water samples were collected at the outlet of the Studibach using automatic samplers (full-size portable sampler, 3712, ISCO Teledyne, USA). The sampling interval was based on the predicted event duration. The multi-interval program was set to sample streamwater every ten to twenty minutes at the start of the rising limb (maximum of six samples). The remaining eighteen samples were taken at an hourly-interval. We emptied the samplers within 24 hours after sample collection to avoid fractionation. We used a timer to start the sampler if the predicted time of the onset of the rainfall was during the night. Rainfall was collected with passive sequential samplers (built after Kennedy et al. (1979), and described in detail in Fischer et al. (2019)) at two locations in the catchment (rain gauge location one and two in Fig. 1a). The samplers collected a sample for approximately every 5 mm of rainfall.

For soil water and groundwater, we used the data from a subset of nine baseflow snapshot campaigns during the snow-free season of 2016 and 2017 (Kiewiet et al., 2019). Soil water was collected with six to 18 suction lysimeters at four to six sites (15, 30 and 50 cm below the surface at forested and non-forested sites at three different elevations: 1361, 1502, 1611 m a.s.l.; Fig.1a). We applied a tension of 50 mbar to the lysimeters and collected the soil water sample the next day. Groundwater was collected at all wells that contained water (34 to 38 wells). The wells were either purged or at least twice the well volume was extracted a day before the sampling. For a detailed description of the groundwater sampling procedure, see Kiewiet et al. (2019).

Ideally we would use the soil water and groundwater samples taken right before the rainfall events, but these data are not available. Instead, we have data from sampling campaigns two to nine days before (event II) or after the events (I, III and IV). Since the spatial variability in groundwater composition in the Studibach is larger than the temporal variability (Kiewiet et al., 2019), we assume that the groundwater and soil water samples reflect the typical composition (and variability) of soil water and groundwater, although absolute concentrations might have been slightly different. A Principal Component Analysis (PCA) on the chemical and isotopic composition of all groundwater (n=335) and soil water (n=116) samples (z-transformed) showed that these were consistently different in the principal component space; only six of the soil water samples (5%) plotted within the same area as the groundwater samples (see S1 for the PCA result and Table 2 for the average concentrations).

3.2 Sample analyses

The samples for cation and anion analyses were stored in the fridge (6 °C) before lab analyses (within a few days) or were frozen (-18 °C) directly after collection until shortly before the analyses. The samples were filtered (0.45 µm; SimplepureTM Syringe Filter) and acidified (only for cation analysis) to mobilize trace metals, and were analysed at the Physics of Environmental Systems laboratory at ETH Zurich. We used an ion-chromatograph (861 Advanced Compact IC, Metrohm) for anions and a mass-spectrometer (ICP-MS 9700, Agilent technologies) for cations. Calibration curves were obtained from measurements with five calibration standards before or after measuring the samples.

The samples were analysed for stable water isotope composition with a Cavity Ring-Down Spectroscope (L2140-I (CRDS) or L2130-I (CRDS), Picarro, Inc., USA) at the Chairs of Hydrology at the University of Freiburg (Germany), with a reported precision of ± 0.16 ‰ for $\delta^{18}O$ and ± 0.6 ‰ for $\delta^{2}H$. All samples plotted close to the local meteoric water line. The average (± standard deviation) of the Line Conditioned-excess (LC-excess; Landwehr and Coplen (2006)) for all 516 stream-, soil- and groundwater samples was 5.3 ± 1.3 ‰, excluding five soil water samples (taken at 15 (three samples), 30 and 50 cm below

https://doi.org/10.5194/hess-2019-686
Preprint. Discussion started: 14 January 2020

Hydrology and Earth System Sciences
Discussions

the soil surface) for which LC-excess ranged from –9.6 to -1.5 ‰. Deuterium-excess (D_{ex}) was calculated as $D_{ex} = \delta^2H - (8 \cdot \delta^{18}O)$.

3.3 Hydrometric measurements

To monitor streamwater and groundwater levels, we used a network of 51 groundwater wells and seven streamflow gauges (Fig.1) that were installed in 2009–2010 (Rinderer et al., 2014). The wells were distributed based on the topographic wetness index (TWI, Beven and Kirkby (1979)) and cover the range of wet and dry locations in the catchment. All wells were drilled by hand to the bedrock (0.5 to 2.5 m depth), screened over the entire length except for the top ten centimeters, and sealed with a bentonite clay. Stream stage was measured directly in the stream (C6 and outlet; Fig. 1a), behind V-notch weirs (C3, C4, and C5) or in H-flumes (C1 and C2). Water levels were measured at each well and stream location with either a capacitance water level logger (Odyssey Dataflow Systems Pty Limited) or a pressure transducer (DCX-22 CTD Keller AG für Druckmesstechnik or STS DL/N 70, Sensor Technick Sirnach AG). The pressure data were corrected for changes in barometric pressure and temperature using the data from the MeteoSwiss station in Einsiedeln (910 m a.s.l; ca. 10 km from the catchment outlet). Rainfall was recorded at three locations within the catchment with tipping bucket rain gauges (0.2 mm resolution, Odyssey Dataflow Systems Pty Limited; Fig.1a).

The stream stage data were converted to specific discharge (Q, further referred to as discharge) using a rating curve based on twenty salt dilution measurements. Due to technical issues, there were no observations of stage height at the catchment outlet during events I and II. We used the correlation between the specific discharge at the catchment outlet and an intermediately sized sub-catchment (C5, Fig.1a) for the four months following events I and II to estimate the streamflow at the outlet for the period without data (coefficient of determination $r^2 = 0.66$, RMSE = 0.75 mm h^{-1}, for comparison the 10th and 90th percentile of Q at the catchment outlet for this period were 0.35 and 2.11 mm h^{-1}, respectively). The ranking of the events based on the peak amount of the (reconstructed) discharge was the same as the ranking based on the peak rainfall intensity, and we therefore assume that the uncertainty in the discharge for events I and II does not affect our conclusions.

3.4 Groundwater-level-based connectivity assessment

We investigated if the assumption of conservative mixing breaks down at a certain specific discharge or hydrologic connectivity. To this end, we related the ratio of the estimated and measured concentrations (C_{Q_x}/C_{es_x}, see 3.5.3) for each solute to the discharge and the calculated fraction of the cachment that was connected to the stream. We used the data-driven model of Rinderer et al. (2019) to determine which parts of the catchment were active and connected to the stream. This model uses the water level data from all 51 wells in the catchment and time series clustering to assign each pixel in the catchment to one of six groundwater level clusters. For each time step, the average relative groundwater level for all monitored wells that belong to a cluster is calculated and assigned to all pixels in that cluster. This relative water level is then transformed to an absolute water level based on the correlation between soil depth and slope. If the water level is within 30 cm of the soil surface (i.e., the part of the soil where the hydraulic conductivity is high), the pixel is considered active, otherwise it is considered inactive. If a pixel is active and, based on surface topography, connected to the stream via other active pixels, it is assumed to be connected to the stream. Rinderer et al. (2019) tested the sensitivity of this method for misclassification of the clusters by randomly re-assigning pixels to different clusters and for the uncertainty in the soil depth by comparing the connectivity timeseries to the timeseries computed with a DEM-based soil map. The soil depth had only minor influence on the model results (RSME > 0.0003% of the relative soil depth), wheareas cluster misclassifications could result in up to 8% difference in the modeled connected area between the different model runs.

https://doi.org/10.5194/hess-2019-686
Preprint. Discussion started: 14 January 2020

205 **3.5 Data analysis**

We investigated the sources of streamflow using two and three-component mixing analyses, and investigated the difference between the observed solute concentrations and those estimated assuming linear mixing of baseflow and rainfall. We examined the changes in streamwater concentrations during the rainfall events using concentration-discharge (C-Q) relationships, and identified the corresponding hysteresis index (Zuecco et al., 2016). For this, we normalized both the discharge and the
210 concentrations so that zero represents the smallest measured value, and one the highest measured value.

We used Mann-Whitney U tests to determine if the median concentrations of different (ground)water types were significantly different (Table 2). We pairwise tested seven groups: all groundwater, riparian groundwater, hillslope groundwater, all soil water, soil water at forested sites, soil water at non-forested sites, and rainfall. We found that the soil water samples taken at
215 forested or non-forested sites were never significantly different, and thus merged these data. We used R (R Core Team, 2013) for all data analyses, and a significance level of 0.05.

3.5.1 Hydrograph Separation and End-Member Mixing Analysis

We estimated the fraction of event (f_e) and pre-event (f_{pe}) water in the stream water samples (C_t) using two-component isotope hydrograph separation (Eq. 1). The results for δ^2H and $\delta^{18}O$ were similar but because the ratio of precision to range was better
220 for δ^2H, we report only the δ^2H results. A pre-event baseflow sample was used to characterize the pre-event water composition (C_{pe}), and the incremental weighted mean of rainfall was used to characterize the event-water composition (C_e).

$$f_{pe} = \frac{C_t - C_e}{C_{pe} - C_e} \qquad (1)$$

225 We also estimated the fractions of groundwater, soil water and rainwater in each streamwater sample, using a three-component End Member Mixing Analysis (EMMA; Christophersen and Hooper (1992)). We based the EMMA on the first two principal components of a PCA that included the isotopic composition and the solutes for which the concentrations in stormflow differed from the concentrations in soil water and groundwater (barium, calcium, magnesium, potassium and sulfate) or which were different for the different groundwater types (copper, manganese and iron).
230

We used a Gaussian error-propagation method (Genereux, 1998) to estimate the uncertainty in the calculated fractions of source waters for the two-component hydrograph separation and EMMA. For the two-component hydrograph separation we defined the uncertainty in the event and pre-event water composition as the standard deviation of the rainfall sampled during the event, and groundwater sampled during the snapshot campaign closest to the event (see Table 1), respectively. For the
235 uncertainty in the EMMA, we used the standard deviation of groundwater, soil water and rain water samples that were used for this particular event. We used the laboratory accuracy for the uncertainty of the streamwater samples in the two-component hydrograph separation, and assumed that the uncertainty for the streamwater samples in the principal component space was minimal.

3.5.2 Relative concentrations

240 For each solute, we calculated relative concentration R_x by comparing the concentration of the sample to that of baseflow:

$$R_x = \frac{C_{Q\_x}}{C_{BF\_x}} \qquad (2)$$

Where C_{Q_x} and C_{BF_x} are the concentration of solute x stream water during the event and in baseflow before the event. The relative concentration indicates dilution (R_x <1) or enrichment ($R_x \geq 1$)) during rain events and thus quantifies the direction and

https://doi.org/10.5194/hess-2019-686
Preprint. Discussion started: 14 January 2020


Hydrology and Earth System Sciences
Discussions

magnitude of the change in solute concentrations (note that R_x is not an alternative measure for the fraction of baseflow in stormflow).

We used the relative concentrations (R_x, Eq. 2) to identify groups of solutes by hierarchical clustering. We then compared the relative concentrations of each solute to that of a conservative tracer to determine any deviation in the relative concentration from conservative mixing between baseflow and rainfall.

3.5.3 Deviation of concentrations from mixing of baseflow and rainfall

The expansion of hydrologically connected areas during events can cause source waters that did not contribute to baseflow to contribute to stormflow. This violates the assumption of simple conservative mixing if baseflow is used to represent the 'old' water (e.g., Hooper, 2001). We therefore compared the measured streamflow concentrations for each solute to the concentration that would be expected based on conservative mixing of rainfall and baseflow using the pre-event water fraction calculated for δ^2H (C_{es}):

$$C_{es\_x} = \left(C_{BF\_x} \cdot f_{pe}\right) + \left(C_{P\_x} \cdot (1 - f_{pe})\right) \quad (3)$$

where C_{es_x} is the 'estimated' concentration for solute x, C_{BF_x} and C_{P_x} are the concentrations for solute x in baseflow and rainfall (average rainfall composition: Table 2), and f_{pe} is the pre-event water fraction for that sample, as determined from the two-component hydrograph separation based on δ^2H (Eq. 1).

We investigated the relation between discharge and the potential contribution of different source areas by comparing the estimated (C_{es_x}) and measured streamflow (C_{Q_x}) concentrations for each sample and solute. We assumed that overestimation of the concentrations ($C_{Q\_x}/C_{es\_x} > 1$) indicates either a contribution from source areas that were not connected during baseflow and have a higher concentration than the sources that contributed to baseflow, or reactive transport. Similarly, underestimation of the concentrations ($C_{Q\_x}/C_{es\_x} < 1$) indicates either a contribution from source areas that were not active during baseflow and have lower concentration than the sources that contributed to baseflow or reactive transport. Given the characteristic concentrations in different (ground)water types (Table 2 and Fig. 2), we assume that higher copper concentrations are indicative of flow from hillslopes and forested areas, higher iron and manganese concentrations are indicative of larger contributions from riparian areas, and higher D_{ex} or barium and chloride concentrations are indicative of soil water (Fig. 2). Lastly, higher potassium concentrations can indicate either soil water or hillslopes contributions, even though we recognize that potassium also has a geogenic origin and is influenced by biological processes.

4. Results

4.1 Event characteristics

Total rainfall for the four events ranged between 17 and 33 mm (Table 1, Fig. 3). All events were larger than the long-term average in daily precipitation and within the upper 30% of daily precipitation at the long-term meteorological station Erlenhöhe, located 500 meters from the catchment outlet (median: 10.0 mm; mean ± sd: 14.1 ± 13.8 mm for all 7452 days with more than 1 mm of precipitation between 1981-2017; Stähli, 2018). However, they were smaller than the 50 mm threshold for large event-water contributions (Fischer et al. 2017). The duration of the events ranged from 7 to 27 hours. The average and maximum 10-minute rainfall intensities ranged between 1.2 and 3.9 mm h^{-1} and between 4.8 and 22.8 mm h^{-1}, respectively.

https://doi.org/10.5194/hess-2019-686
Preprint. Discussion started: 14 January 2020

Hydrology and Earth System Sciences
Discussions

Discharge at the catchment outlet increased the least (0.02 to 0.07 mm h^{-1}) for the smallest event (I), and most for event III (0.08 to 0.43 mm h^{-1}). The modelled fraction of the catchment that was hydrologically connected varied from 0.27 (before the start of event I and II) to 0.68 (during peak flow of event III) (Fig. 4). The relation between the fraction of the catchment that was connected to the stream and discharge was non-linear for all events (Fig. 5, top row). For event I the connected area increased significantly at the recession of the streamflow, whereas for event II connectivity increased little during the sampling period (0.27 to 0.28). Interestingly, discharge increased to >4 mm h^{-1} after the sampling period of event II due to additional rainfall, whereas connectivity increased only marginally (up to 0.35; see S2). During these periods of relatively low connectivity, the hydrologically connected area extended laterally from the stream up, but remained confined to the flat areas. For the intermediate events (III and IV), the lateral extension was larger and parts of the hillslopes became connected. However, the data based model suggested that during all events, large parts of the catchment remained hydrologically disconnected (Table 1).

4.2 Concentration-discharge relationships

The chemical and isotopic composition of streamwater changed during all events, but the magnitude and direction of the response differed for each event and solute (Fig. 5). The change in the concentrations was smallest during event I (e.g., a maximum change of 7.7 mg L^{-1} for Ca and 15.8 µg L^{-1} Fe) and largest for event III (a maximum change of 39 mg L^{-1} and 72.9 µg L^{-1} for Ca and Fe, respectively). Hysteresis in the relation between solute concentrations and discharge depended on the event size and differed between solutes (Table 3, Fig. 5). During event III and IV the relation between discharge and concentration was hysteretic for most solutes. The double discharge peaks during events I and II (Fig. 2) resulted in a double loop in the concentration discharge relationship for deuterium and iron (Fig. 5).

The average relative concentration (average R_x for all the samples from all four events, n=100, Eq. 2) for deuterium excess (D_{ex}) and chloride were 4.1 and 2.0, respectively. This reflects the substantial increase in these concentrations during events. Manganese and iron concentrations also increased with increasing discharge, but less than D_{ex} and chloride (mean R_x: 1.0 for both iron and manganese; maximum R_x: 2.8 and 3.2, respectively). On average, the concentrations of copper, nickel and zinc decreased with increasing discharge (mean R_x: 0.78, 0.63 and 0.31), but individual stormflow samples were enriched up to 1.7, 1.3 and 1.1 times the baseflow concentration, respectively. Concentrations of iron and copper were always higher on the falling limb than on the rising limb (counter-clockwise hysteresis). Event I was the only event during which copper concentrations did not increase from the baseflow concentration.

The concentrations of sodium, magnesium, calcium and barium decreased with increasing discharge (mean R_x: < 0.77). The concentrations of these solutes, and also sulfate, were higher on the rising limb than on the falling limb (resulting in clockwise hysteresis). Sulfate concentrations decreased with increasing discharge during events I, III and IV but increased with discharge during event II. Potassium and sulfate concentrations (range R_x: 0.2–1.7 and 0.3–1.4, respectively), were highest shortly after the onset of an event (first four samples), and decreased afterwards. These differences in the magnitude and timing of the change in solute concentrations and isotopic composition allowed for subdivision of the solutes into different groups (A to D; Table 3, Fig. 6) based on the computed R_x values for all events.

4.3 Hydrograph Separation and End Member Mixing Analysis

Two-component hydrograph separation results indicated that most stormflow was ‘old’ water (Fig. 3; Table 3). The maximum event water fraction (f_e) was highest for event II (f_e = 0.24±0.31) and smallest for event IV (f_e = 0.03±0.19). The high event water fraction of event II occurred when the connected area was relatively small. The fraction of connected area during event II expanded only 0.01 (up to 0.28) during the period that we sampled (see S2). The high event-water fractions for event III,

https://doi.org/10.5194/hess-2019-686
Preprint. Discussion started: 14 January 2020

compared to the similarly sized event IV, might be the result of the much smaller hydrologically connected area and relatively high peak rainfall intensity ($I_{p\text{-}max}$: 24 mm h^{-1} vs 10 mm h^{-1} for event IV, Table 1).

The explanatory power of the first two principal components, for all stormflow, soil water and groundwater samples was 41.9% for event I (PC1: 26.0%; PC2: 15.9%) and 43.2% for event III (PC1: 27.0%; PC2: 16.2%; Fig. 7a and c). For event II and IV the explanatory power was 41.1% and 49.0%, respectively; see S3). The principal component axes were most strongly determined by the calcium concentrations (orientation close to PC1 for both events), the isotopic composition (more so in event III) and to a lesser extent concentrations of copper, magnesium, potassium, and deuterium-excess (Fig. 7a and c). It was possible to calculate the relative fractions of groundwater, soil water and rainwater in stormflow for all events but the calculated uncertainties were very large (Table 4). Groundwater fractions (f_{GW}) were larger than rainwater and soil water fractions for events I, III and IV (range f_{GW}: 0.39±1.59 to 0.72±1.43). During event II, the rainwater fraction was largest (fraction rainwater: 0.45±0.60; soil water: 0.33±0.60; groundwater: 0.21±0.60). Event-average soil water fractions were negligible (f_{SW} ~0) during events I and IV (Table 4). The event-average pre-event water fractions based on the end-member mixing analysis (the sum of the groundwater and soil water fractions) was lower than the pre-event water fraction estimated using δ^2H as a tracer in the two-component hydrograph separations (range $f_{GW} + f_{SW}$: 0.54 to 0.77 vs range f_{pe}: 0.76 to 0.97).

The most striking aspect of the mixing plots is the small change in the composition of stormflow compared to the spatial variation in the composition of the end-members (Fig. 7b and d). The observed changes in solute concentrations in streamflow were largest during event III (e.g., changes of 25 μgL^{-1} for Ba; 39 mgL^{-1} for Ca and 5 ‰ for δ^2H) but this change was similar to the standard deviation of the concentrations for all the groundwater samples (44 μgL^{-1} for Ba, 27 mgL^{-1} for Ca and 5.9 ‰ for δ^2H). This resulted in high uncertainties in the calculated fractions (Table 4), and inhibits robust interpretation regarding the source areas.

4.4 Estimated solute concentrations based on conservative mixing of rainfall and baseflow

The concentrations estimated based on the assumption of conservative mixing between rainfall and baseflow (C_{es}, Eq. 3) differed from the measured stormflow concentrations (C_Q) for almost all solutes (Fig. 8). The measured concentrations for geogenic solutes (shown for calcium and sodium in Fig. 8a and b) were lower than the estimated concentrations. This could be due to mixing with a source with lower calcium or sodium concentrations (for instance soil water, or other contributions from the riparian areas; Table 2). The measured concentrations of sulfate (Fig. 8c) were lower than estimated based on conservative mixing for event I, III and IV. For potassium concentrations there was no clear pattern: the concentrations were underestimated and overestimated at both lower and higher discharges (Fig. 8d), which is probably due to the high variation in soil water and groundwater potassium concentrations (Table 2). The measured concentrations of cobalt, copper, nickel and iron (group A and C) were slightly lower than the estimated concentrations for low discharge but (much) higher during high discharge (Fig. 8e-h). For copper and nickel this could be due to hillslope contributions, whereas for iron and cobalt it could be due to increased contributions from the riparian areas (see Table 2 and Table 3 for (ratios of) concentrations in different groundwater sources, as well as soil water and groundwater). There was no distinct threshold in the relation between C_Q/C_{es} and either discharge or the fraction of the catchment that was connected (Fig. 8 and S4).

5. Discussion

5.1 Small changes in streamflow composition compared to the spatial variability

Changes in solute concentrations in streamwater during rainfall events depend on changes in the relative contributions of different sources to streamflow (e.g., event and pre-event water, or different pre-event water sources), as well as reactive

https://doi.org/10.5194/hess-2019-686
Preprint. Discussion started: 14 January 2020

transport processes. Our results show that the change in streamflow composition during the four rainfall events was smaller than the spatial variability in groundwater and soil water composition. For instance, the change in the concentration of barium and deuterium in streamflow for the event with the largest changes was similar to the spatial variability in shallow groundwater and soil water measured after that event (25 μgL^{-1} barium and 5.0 ‰ change in stream water, versus an interquartile range of 30 μgL^{-1} and 4.8 ‰ for shallow groundwater and 10.6 mgL^{-1} and 5.7 ‰ in soil water). This was also evident from the principal component analysis and mixing plots (Fig. 7). For a viable hydrograph separation, the change in streamwater composition should be larger than the variability within the end-members (Hooper, 2001). This was not the case for the Studibach catchment and thus the change in stream water composition was not large enough to distinguish contributions from different (groundwater) sources, but the results did indicate that soil water fractions were considerable (about 0.3 to 0.4) for two out of the four events (Table 4).

We could show that the spatial variation within different source areas is large compared to the temporal variation, since we had a large dataset of groundwater and soil water samples available. However, in other small catchment studies this comparison is often restricted, because of insufficient spatial sampling (Penna and van Meerveld, 2019). Hence, in order to find out if the spatial variation is also larger than the temporal variation in other locations (or if it is not), it is paramount to quantify the spatial variation by sampling groundwater and soil water at multiple sites in more research areas. Then we will also know if the uncertainties (Table 4) are extreme or also typical for other catchments.

The importance of soil water confirms earlier findings by Hagedorn et al. (2000), who analysed three rainfall events (7 mm, 8 mm and 30 mm rainfall) in the neighbouring Erlenbach catchment. The mixing diagrams using chloride and calcium in their study indicate that the average contribution of the top soil was larger than 50%. However, chloride and calcium concentrations vary considerably in both soil and groundwater (average coefficient of variation: 0.86 and 1.0 for eight soil water (n=6 to 18) and 1.0 and 0.3 for nine groundwater (n=34 to 47) snapshot campaigns for chloride and calcium respectively). Furthermore, bivalent cations, like calcium, can increase rapidly in throughfall through canopy leaching (Lindberg et al., 1986). Moreover, van Meerveld et al. (2018) found that calcium concentrations in overland flow from small landslide areas in the Studibach were much higher than for other solutes, indicating rapid dissolution.

5.2 Which areas contribute to stormflow?

The presence of different ‘old’ water stores in the catchment, which are mobilized in different proportions at high and low flows, can cause changes in stream water composition during events (Kirchner, 2003). To illustrate this, we tested if simple mixing of baseflow and rainfall could explain the solute concentrations in stream water during events. We found that the measured and expected concentrations differed for most solutes (Fig. 8). Concentrations of metals, such as iron or copper, were much higher than expected from mixing of rainfall and baseflow, whereas weathering-derived solutes, such as sodium or calcium, were lower than expected. We interpret the differences between the measured and expected concentrations, particularly on the falling limb and at peak flow, to be at least partly caused by contributions from soil water or groundwater sources that did not contribute to baseflow (see Table 3 for ratios of concentrations in different source waters). For instance, the differences for weathering-derived solutes could be due to contributions from soil water, which has lower concentrations of these solutes than groundwater. The concentrations of iron increased throughout the event until peakflow and were higher on the falling limb than on the rising limb. Since riparian groundwater has relatively high concentrations of iron (Table 2 and 3), elevated contributions from riparian areas throughout the rainfall events could explain this increase. Measured copper concentrations were much higher than expected for event III and IV, but lower than expected for event I and II. Because copper concentrations are relatively high on the hillslopes and low in soil water (Table 2 and 3; Kiewiet et al., 2019), this could be an indication that the hillslopes did not actively contribute to streamflow during these events, and were only activated after peak

https://doi.org/10.5194/hess-2019-686
Preprint. Discussion started: 14 January 2020

flow (see wide hysteresis for event I in Fig. 5, top row). However, then the copper concentrations should also not have increased relative to baseflow during event II, which was not strictly the case (maximum R_{Cu} during event II: 1.7 vs 1.0, 1.0 and 1.4 during event I, III and IV, respectively). In any case, the solute concentrations could not be explained as the simple mixture of rainfall and baseflow for any of the events, but the differences between the expected and measured concentrations can at least partly be explained by contributions from other (groundwater) source areas.

For the events included in this study, the area estimated to be hydrologically connected was never smaller than a quarter of the entire catchment area, increased laterally upslope from the stream, and reached a maximum of 0.68 of the entire catchment area. The simulated connected area during a relatively small event (event I, total rainfall 17 mm) increased by 0.20, which implies that little precipitation can activate large parts of the catchment. The simulations of the active and connected stream network confirm that the near-stream areas are most often connected and respond first to rainfall, which shows their importance for the rapid generation of streamflow (Fig. 4). The difference between the expected and measured concentrations (Fig. 8) also suggests that the quick increase in connected area is important: even for small increases in discharge, stormflow could not be described as a mixture of rainfall and baseflow. However, the connectivity simulations for event II suggest that connectivity can change little during long, low-intensity rainfall events. This might be reflected in the higher soil water and rainfall fractions in stormflow for event II, whereas typically groundwater dominates streamflow in this catchment.

Given the typically moderate event-water fractions, we expect that surface runoff is likely to be of minor importance for streamflow, although surface runoff does occur in the Studibach (van Meerveld et al., 2018). Alternatively, it may have infiltrated through macropores or unsaturated soils before reaching the stream. This corresponds to the event-water fractions based on the two-component hydrograph separation (event-average event water fraction: 0.03±19 to 0.24±0.31), but less with the EMMA results (range: 0.25±1.24 to 0.47±0.40, Table 3), and indicates that contributions from other sources than rainfall are likely important.

Despite large changes in the hydrologically connected area and the large spatial variability in groundwater composition, we did not observe a distinct threshold in the deviation of stream chemistry from simple conservative mixing of rainfall and baseflow. This gradual change might be caused by the (relatively) gradual increase in the connected area with increasing discharge for all events, except event I, for which the connectivity increased abruptly after peak discharge (top row in Fig. 5). Alternatively, the change in stormflow composition could be the result of the mixing of a large number of source areas. Abbott et al. (2018) showed that the change in streamflow composition with increasing discharge and connectivity is less pronounced for catchments with a myriad of source areas than for catchments with fewer different landscape elements. The Studibach is characterized by many small landscape elements, particularly steep hillslopes and flat, wet areas, which formed due to landslides and soil creep and induced small-scale differences in soil and vegetation development. Hence, activation of different landscape elements might occur semi-simultaneously at different places across the catchment (i.e., the connected area extends from flat locations to the hillslopes at many different transects), but the outflows of these elements mix on its way down to the outlet. From this perspective, it is not surprising that solute concentrations in stormflow changed little compared to the spatial variability in the end-member composition. Streamflow is a mixture of different water sources in a heterogeneous catchment.

6. Conclusions

The results of this study showed that the spatial variability in soil water and groundwater composition across a small pre-alpine headwater catchment is larger than the temporal variation in stream water during events. This resulted in very large uncertainties in the estimated source water fractions. Groundwater was the dominant source of streamflow for three of the four

https://doi.org/10.5194/hess-2019-686
Preprint. Discussion started: 14 January 2020

Hydrology and Earth System Sciences
Discussions

events. Soil water contributions were very small for two events. The stream water concentrations could not be explained by conservative mixing of baseflow and rainfall for most solutes. The differences were largest at high discharge, indicating that this may be caused by the contributions from other sources due to the expansion of the connected area. However, there was no threshold in the relation between the deviations of the concentrations from the expected concentrations based on mixing, suggesting that there was no sudden activation of source areas to cause the observed changes in concentrations. Instead, the gradual changes in solute concentrations are likely the result of increases in the contributions from many (small) landscape elements in the catchment and the gradual increase in connectivity during events. The modelled hydrologically connected area and changes in solute concentrations both suggest that source areas change during events. This highlights the importance of characterizing the composition of different source areas, and the spatial variability within these areas when using stream-based measurements to investigate hydrologic connectivity.

Data availability

The data that support the findings of this study are available from the corresponding author upon reasonable request.

Author contributions

LK and IVM conceptualized the study. LK collected and analysed the data, and prepared the manuscript. IVM, JS and MS provided recommendations for the data analysis, participated in discussions about the results, and revised the manuscript.

Competing interests

The authors declare that they have no competing interests.

Acknowledgements

This work would not have been possible without the help and support of many people in the field and lab. We particularly thank Michael Rinderer and Benjamin Fischer for the initial installation of the wells, weirs and flumes, Michael Rinderer for running the data-based connectivity model for the Studibach; Barbara Herbstritt for the isotope analyses, and Bjorn Studer for the cation and anion analyses. We thank Oberallmeindkorporation Schwyz (OAK), the municipality of Alpthal, and the Department of Environment of the Canton of Schwyz for the excellent cooperation.

References

Abbott B. W., Gruau G., Zarnetske J. P., Moatar F., Barbe L., Thomas Z., Fovet O., Kolbe T., Gu S., Pierson-Wickmann A. C., et al., Unexpected spatial stability of water chemistry in headwater stream networks, Ecol. Lett., 21, 296–308, https://doi.org/10.1111/ele.12897, 2018.

Allaire S. E., Sylvain C., Lange S. F., Thériault G., Lafrance P., Potential Efficiency of Riparian Vegetated Buffer Strips in Intercepting Soluble Compounds in the Presence of Subsurface Preferential Flows, PloS One, 10, 1–21 https://doi.org/10.1371/journal.pone.0131840, 2015.

Barthold F. K., Tyralla C., Schneider K., Vaché K. B., Frede H. G., Breuer L., How many tracers do we need for end member mixing analysis (EMMA)? A sensitivity analysis, Water Resour. Res., 47, 1–14, https://doi.org/10.1029/2011WR010604, 2011.

Beven K. J., Kirkby M. J., A physically based, variable contributing area model of basin hydrology, Hydrol. Sci. J., 24, 43–69 https://doi.org/10.1080/02626667909491834, 1979.

Blume T., van Meerveld H. J. I., From hillslope to stream: methods to investigate subsurface connectivity, WIREs Water 2, 177–198 https://doi.org/10.1002/wat2.1071, 2015.

Bracken L. J., Croke J., The concept of hydrological connectivity and its contribution to understanding runoff-dominated geomorphic systems, Hydrol. Process., 21, 2267–2274, https://doi.org/10.1002/hyp.6313, 2007.

Brown V. A., McDonnell J. J., Burns D. A., Kendall C., The role of event water, a rapid shallow flow component, and catchment size in summer stormflow, J. Hydrol., 217, 171–190, https://doi.org/10.1016/S0022-1694(98)00247-9, 1999.

Burns, D. A., Hooper, R. P., McDonnell, J. J., Freer, J. E., Kendall, C., and Beven, K., Base cation concentrations in subsurface flow from a forested hillslope: The role of flushing frequency, Water Resour. Res. 34, 3535– 3544, https://doi.org/10.1029/98WR02450, 1998.

Buttle, J. M., Isotope hydrograph separations and rapid delivery of pre-event water from drainage basins, Prog. Phys. Geogr. 18, 16–41. https://doi.org/10.1177/030913339401800102, 1994.

Christophersen N., Hooper R. P., Multivariate Analysis of Stream Water Chemical Data' The Use of Principal Components Analysis for the End-Member Mixing Problem, Water Resour. Res., 28, 99–107, https://doi.org/10.1029/91WR02518, 1992.

Detty J. M., McGuire K. J., Threshold changes in storm runoff generation at a till - mantled headwater catchment, Water. Resour. Res., 46, 1–15, https://doi.org/10.1029/2009WR008102, 2010.

Devito K. J., Hill A. R., Sulphate dynamics in relation to groundwater - Surface water interactions in headwater wetlands of the southern Canadian Shield, Hydrol. Process., 11, 485–500, https://doi.org/10.1002/(sici)1099-1085(199704)11:5<485::aid-hyp455>3.0.co;2-f, 1997.

Evans C., Davies T. D., Causes of concentration/discharge hysteresis and its potential as a tool for analysis of episode hydrochemistry, Water Resour. Res., 34, 129–137, https://doi.org/10.1029/97WR01881, 1998.

Feyen H., Wunderli H., Wydler H., Papritz A., A tracer experiment to study flow paths of water in a forest soil, J. Hydrol., 225, 155–167, https://doi.org/10.1016/S0022-1694(99)00159-6, 1999.

Fischer B., Aemisegger F., Graf P., Sodemann H., Seibert J., Assessing the Sampling Quality of a Low-Tech Low-Budget Volume-Based Rainfall Sampler for Stable Isotope Analysis. Front. Earth Sci. 7, 1-8, https://doi.org/10.3389/feart.2019.00244, 2019.

Fischer B. M. C., Rinderer M., Schneider P., Ewen T., Seibert J., Contributing sources to baseflow in pre-alpine headwaters using spatial snapshot sampling, Hydrol. Process., 29, 5321–5336, https://doi.org/10.1002/hyp.10529, 2015.

Fischer B. M. C., Stähli M., Seibert J., Pre-event water contributions to runoff events of different magnitude in pre-alpine headwaters, Hydrol. Res., 48, 28–47, https://doi.org/10.2166/nh.2016.176, 2017.

von Freyberg J., Radny D., Gall H. E., Schirmer M., Implications of hydrologic connectivity between hillslopes and riparian zones on streamflow composition, J. Contam. Hydrol., 169, 62–74, https://doi.org/10.1016/j.jconhyd.2014.07.005, 2014.

von Freyberg J., Studer B., Rinderer M., Kirchner J. W., Studying catchment storm response using event- and pre-event-water volumes as fractions of precipitation rather than discharge, Hydrol. Earth Syst. Sci., 22, 5847–5865 https://doi.org/10.5194/hess-22-5847-2018, 2018.

Genereux D., Quantifying uncertainty in tracer-based hydrograph separations, Water Resour. Res., 34, 915–919 https://doi.org/10.1029/98WR00010, 1998.

Godsey S. E., Kirchner J. W., Clow D. W., Concentration – discharge relationships reflect chemostatic characteristics of US catchments, 23, 1844–1864, https://doi.org/10.1002/hyp.7315, 2009.

Hagedorn F., Schleppi P., Waldner P., Flühler H.. Export of dissolved organic carbon and nitrogen from Gleysol dominated catchments--the significance of water flow paths, Biogeochem., 50,137–161, https://doi.org/10.1023/A:1006398105953, 2000.

Hooper R. P., Applying the scientific method to small catchment studies: a review of the Panola Mountain experience, Hydrol. Process., 15, 2039–2050, https://doi.org/10.1002/hyp.255, 2001.

Hooper R. P., Christophersen N., Peters N. E., Modelling streamwater chemistry as a mixture of soilwater end-members - An application to the Panola Mountain catchment, Georgia, U.S.A., J. Hydrol., 116, 321–343, https://doi.org/10.1016/0022-1694(90)90131-G, 1990.

Hopp L., McDonnell J. J., Connectivity at the hillslope scale: Identifying interactions between storm size, bedrock permeability, slope angle and soil depth, J. Hydrol., 376, 378–391, https://doi.org/10.1016/j.jhydrol.2009.07.047, 2009.

Hornberger G. M., Scanlon T. M., Raffensperger J. P., Modelling transport of dissolved silica in a forested headwater catchment: the effect of hydrological and chemical time scales on hysteresis in the concentration – discharge relationship, Hydrol. Process., 15, 2029–2038, https://doi.org/10.1002/hyp.254, 2001.

Jencso K. G., McGlynn B. L.., Hierarchical controls on runoff generation: Topographically driven hydrologic connectivity, geology, and vegetation, Water Resour. Res., 47, 1–16, https://doi.org/10.1029/2011WR010666, 2011.

Kaushal S. S., Gold A. J., Bernal S., Newcomer Johnson T. A., Addy K., Burgin A., Burns D. A., Coble A. A., Hood E., Lu Y., et al., Watershed 'chemical cocktails': forming novel elemental combinations in Anthropocene fresh waters, Biogeochem., 141, 281–305, https://doi.org/10.1007/s10533-018-0502-6, 2018.

Kennedy V. C., Zellweger G. W., Avanzino R. J.., Variation of rain chemistry during storms at two sites in northern California, Water Resour. Res., 15, 687–702, https://doi.org/10.1029/WR015i003p00687, 1979.

Kiewiet L., von Freyberg J., van Meerveld H. J. I., Spatiotemporal variability in hydrochemistry of shallow groundwater in a small pre-alpine catchment: The importance of landscape elements, Hydrol. Process., 1–21, https://doi.org/10.1002/hyp.13517, 2019.

Kiewiet L., van Meerveld I., Seibert J., Effects of spatial variability in the groundwater isotopic composition in a pre-alpine headwater catchment on hydrograph separation results, in review.

Kirchner J. W., A double paradox in catchment hydrology and geochemistry, Hydrol Process., 17, 871–874 https://doi.org/10.1002/hyp.5108, 2003.

Ladouche B., Probst A., Viville D., Idir S., Baqué D., Loubet M., Probst J. L., Bariac T., Hydrograph separation using isotopic, chemical and hydrological approaches (Strengbach catchment, France), J. Hydrol., 242, 255–274, https://doi.org/10.1016/S0022-1694(00)00391-7, 2001.

Landwehr J. M., Coplen T. B., Line-conditioned excess: A new method for characterizing stable hydrogen and oxygen isotope ratios in hydrologic systems (IAEA-CSP--26/P), 2006.

Lehmann P., Hinz C., McGrath G., Tromp-van Meerveld H. J., McDonnell J. J., Rainfall threshold for hillslope outflow: an emergent property of flow pathway connectivity, Hydrol. Earth Syst. Sci., 11, 1047–1063, https://doi.org/10.5194/hessd-3-2923-2006, 2007.

Lindberg S. E., Lovett G. M., Richter D. D., Johnson D. W., Atmospheric Deposition and Canopy Interactions of Major Ions in a Forest, Science, 231, 141–145, https://doi.org/10.1126/science.231.4734.141, 1986.

McGlynn B. L., McDonnell J. J., Quantifying the relative contributions of riparian and hillslope zones to catchment runoff, Water Resour. Res., 39, 1310, https://doi.org/10.1029/2003WR002091, 2003.

van Meerveld H. J., Seibert J., Peters N. E., Hillslope-riparian-stream connectivity and flow directions at the Panola Mountain Research Watershed, Hydrol. Process., 29, 3556–3574, https://doi.org/10.1002/hyp.10508, 2015

van Meerveld H. J. I., Fischer B. M. C., Rinderer M., Stähli M., Seibert J., Runoff generation in a pre-alpine catchment: A discussion between a tracer and a shallow groundwater hydrologist, Cuad. de Investig. Geogr., 44, 429–452, https://doi.org/10.18172/cig.3349, 2018.

https://doi.org/10.5194/hess-2019-686
Preprint. Discussion started: 14 January 2020

Ocampo C. J., Sivapalan M., Oldham C., Hydrological connectivity of upland-riparian zones in agricultural catchments: Implications for runoff generation and nitrate transport, J. Hydrol., 331. 643–658, https://doi.org/10.1016/j.jhydrol.2006.06.010, 2006.

Oswald C. J., Richardson M. C., Branfireun B. A., Water storage dynamics and runoff response of a boreal Shield headwater catchment, Hydrol. Process., 25, 3042–3060, https://doi.org/10.1002/hyp.8036, 2011.

Penna D., van Meerveld H. J., Spatial variability in the isotopic composition of water in small catchments and its effect on hydrograph separation, WIREs Water, 1–33, https://doi.org/10.1002/wat2.1367, 2019.

R Core Team, R: A language and environment for computing. R Foundation for Statistical Computing, Vienna, Austria, Available at: http://www.r-project.org/, 2013.

Rinderer M., van Meerveld H. J. I., McGlynn B., From Points to Patterns: Using Groundwater Time Series Clustering to Investigate Subsurface Hydrological Connectivity and Runoff Source Area Dynamics, Water Resour. Res. 55, 1–23 https://doi.org/10.1029/2018WR023886, 2019.

Rinderer M., van Meerveld H. J., Seibert J., Topographic controls on shallow groundwater levels in a steep, prealpine catchment. Water Resour. Res., 50, 6067–6080, https://doi.org/.1002/2013WR015009, 2014.

Rinderer M., van Meerveld I., Stähli M., Seibert J., Is groundwater response timing in a pre-alpine catchment controlled more by topography or by rainfall?, Hydrol. Process., 30, 1036–1051, https://doi.org/10.1002/hyp.10634, 2015.

Seibert J., Grabs T., Köhler S., Laudon H., Winterdahl M., Bishop K., Linking soil-and stream-water chemistry based on a Riparian Flow-Concentration Integration Model, Hydrol. Earth Syst. Sci, 13, 2287–2297, https://doi.org/10.5194/hessd-6-5603-2009, 2009.

Stähli M., Longterm hydrological observatory Alptal (central Switzerland). Available at: https://www.envidat.ch/dataset/longterm-hydrological-observatory-alptal-central-switzerland, 2018.

Stähli M., Gustafsson D., Long-term investigations of the snow cover in a subalpine semi-forested catchment, Hydrol. Process., 20, 411–428, https://doi.org/10.1002/hyp.6058, 2006.

Stieglitz M., Shaman J., McNamara J., Engel V., Shanley J., Kling G.W., An approach to understanding hydrologic connectivity on the hillslope and the implications for nutrient transport. Global Biogeochem. Cycles 17, https://doi.org/10.1029/2003GB002041, 2003.

Zuecco G., Penna D., Borga M., van Meerveld H. J., A versatile index to characterize hysteresis between hydrological variables at the runoff event timescale, Hydrol. Process., 1449–1466, https://doi.org/10.1002/hyp.10681, 2016.

Zuecco G., Rinderer M., Penna D., Borga M., van Meerveld H. J., Quantification of subsurface hydrologic connectivity in four headwater catchments using graph theory, Sci. Total Environ., 646, 1265–1280 https://doi.org/10.1016/j.scitotenv.2018.07.269, 2019.

https://doi.org/10.5194/hess-2019-686
Preprint. Discussion started: 14 January 2020

Hydrology and Earth System Sciences
Discussions
Open Access
EGU

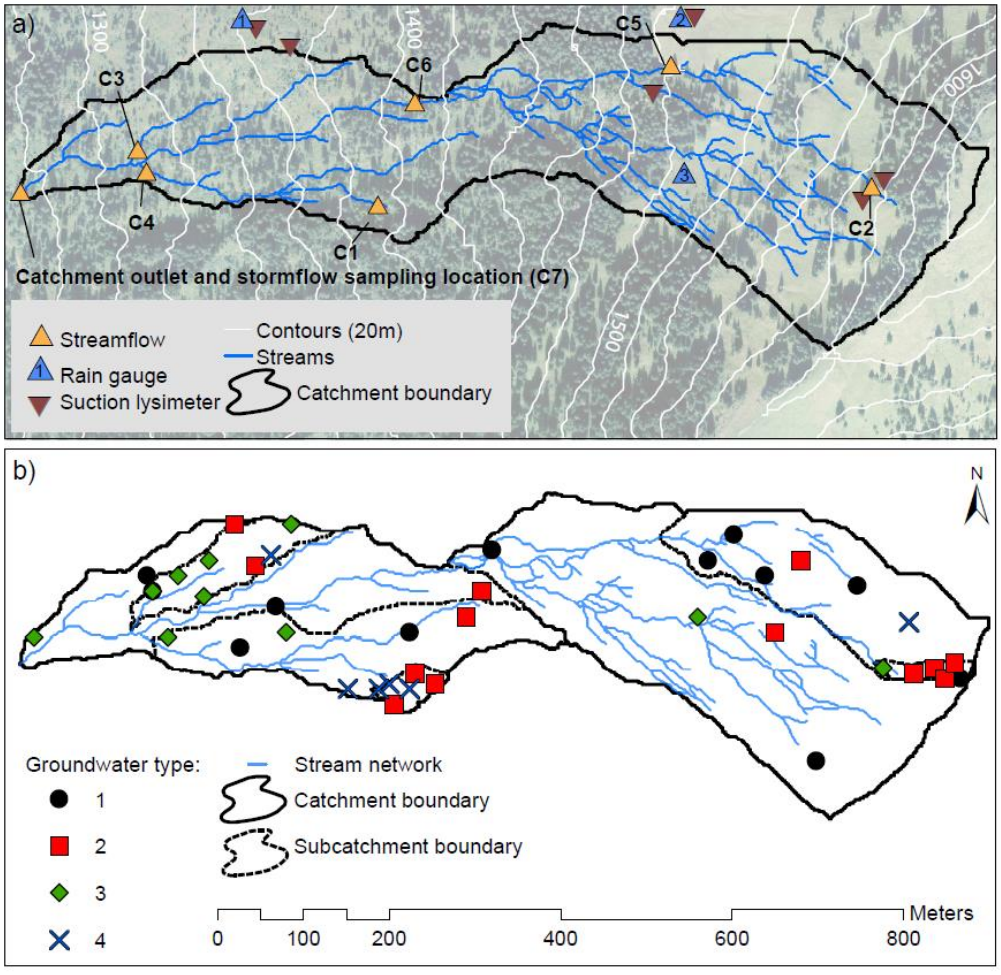

600 **Figure 1. Maps of the Studibach catchment with a) the stream network (blue lines), stream gauges (orange triangles), rain gauges (blue triangles, 1 – 3) and suction lysimeters (brown reversed triangles), 20 m contour lines (white) and the catchment boundary (black); b) sub-catchment boundaries (dashed lines) and location of the wells, color coded by groundwater type 1. riparian wells; 2. hillslope wells; 3. 'deep' groundwater wells; 4. wells with high magnesium and sulfate concentration based on Kiewiet et al. (2019).**

https://doi.org/10.5194/hess-2019-686
Preprint. Discussion started: 14 January 2020

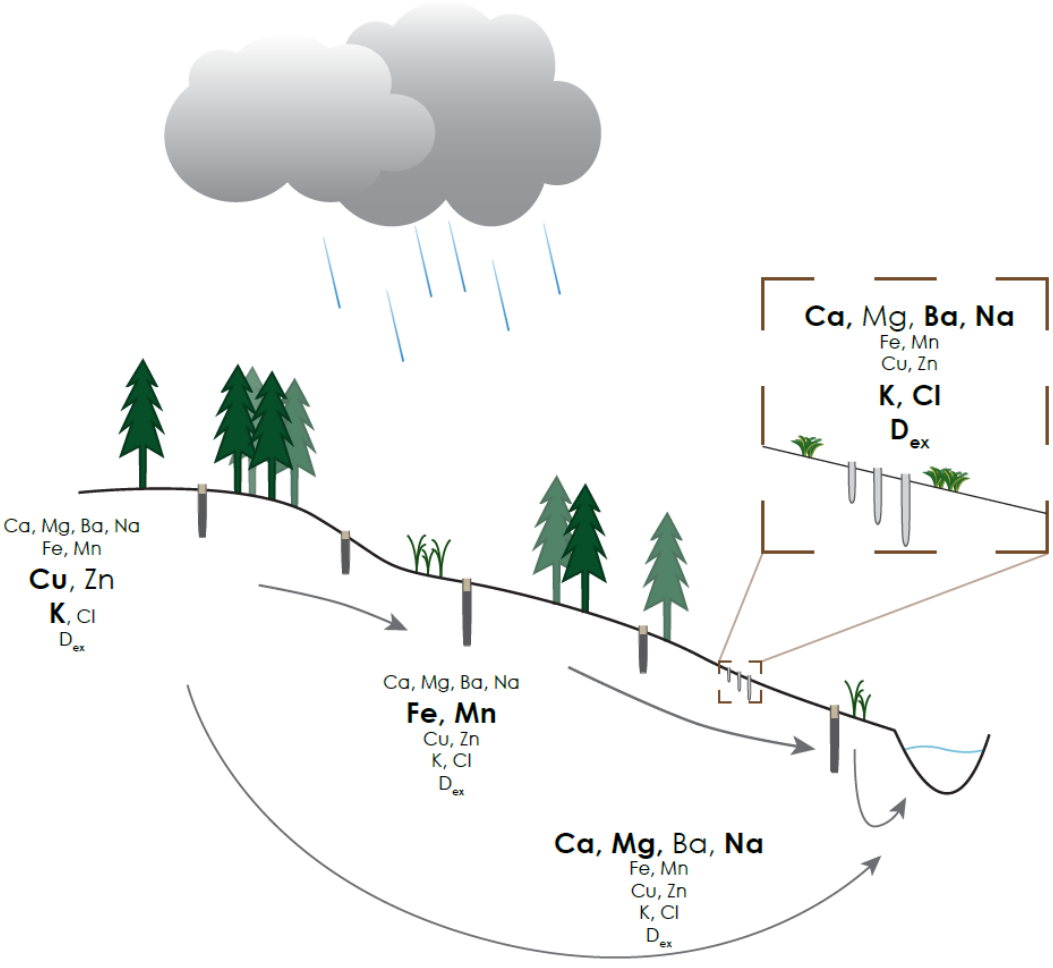

Figure 2. Illustration of a hillslope cross-section with different (ground)water compartments (based on Kiewiet et al., 2019 and Table 2), showing the tracers used in combination with δ^2H and $\delta^{18}O$ to characterize source areas. For most elements, the concentrations were low in rainfall compared to the concentrations in the other water compartments. High potassium, barium and chloride concentrations and high deuterium excess are indicative of soil water. For shallow groundwater, the concentrations of copper and potassium were higher at (forested) ridge locations, whereas for sites with water tables that are persistently close to the surface, the concentrations of iron and manganese were higher. We assume that higher concentrations of geogenic solutes (calcium, magnesium and sodium) indicate longer subsurface residence times. The isotopic composition for the different water compartments depends on the composition of recent and current precipitation.

https://doi.org/10.5194/hess-2019-686
Preprint. Discussion started: 14 January 2020

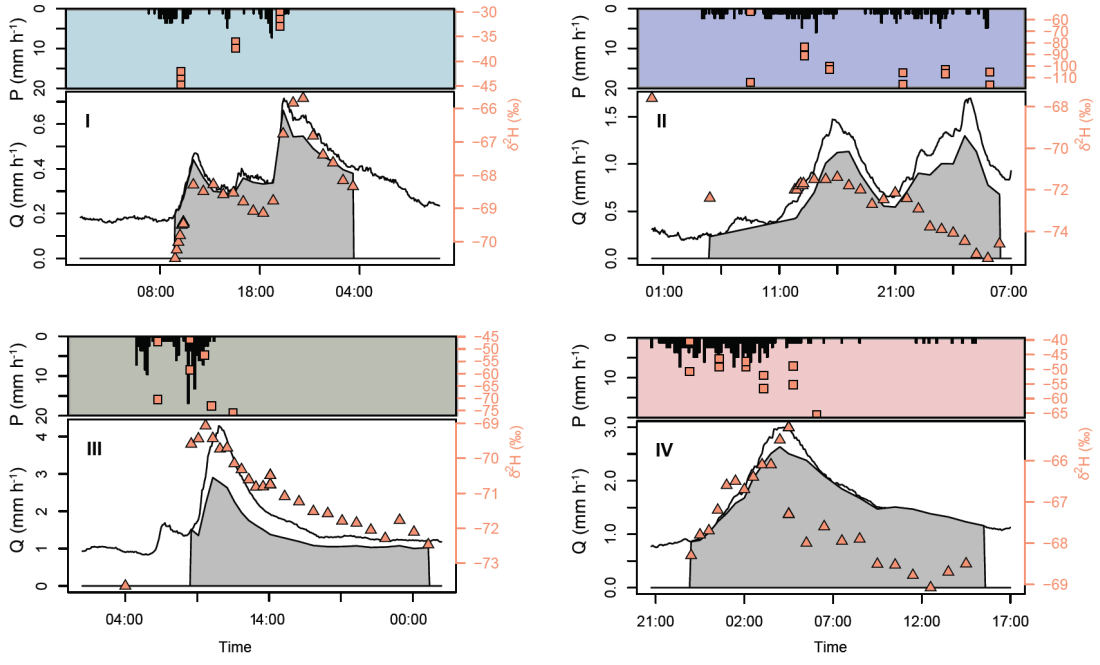

615 **Figure 3. Hydrographs and hyetographs for the four events (I – IV). For each event, the upper panel shows the 10-min rainfall intensity (mm h^{-1}, bar graph) and the isotopic composition of the rainfall (δ^2H in ‰, orange squares), while the lower panel shows the discharge at the catchment outlet (mm h^{-1}, solid line), the isotopic composition of stream water (δ^2H in ‰, orange triangles), and the pre-event water fraction of streamflow based on two-component hydrograph separation using δ^2H (grey polygon) as a tracer.**

https://doi.org/10.5194/hess-2019-686
Preprint. Discussion started: 14 January 2020

Hydrology and Earth System Sciences
Discussions
Open Access
EGU

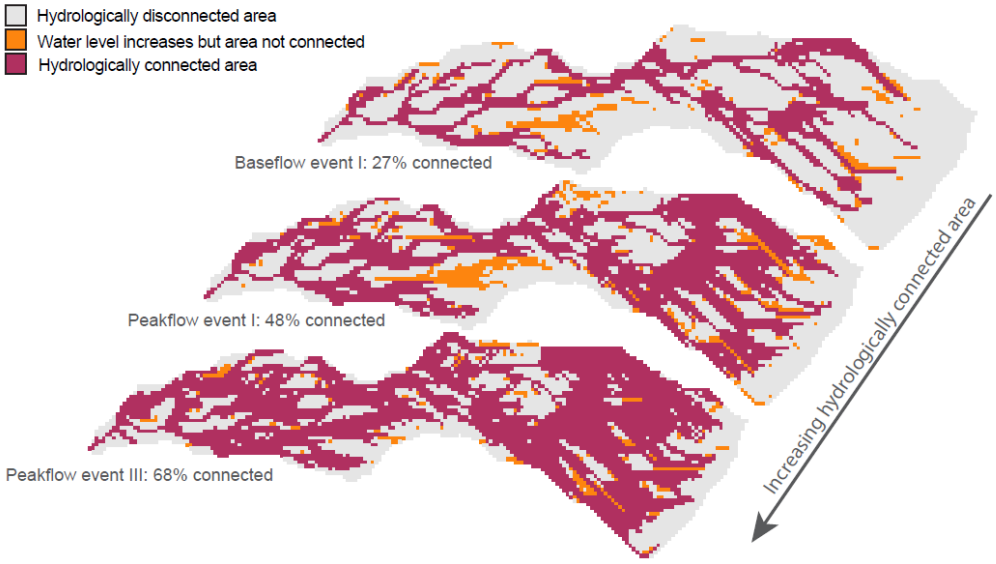

620

Figure 4. The simulated spatial pattern of the hydrologically connected area for three different flow conditions: from relatively low flow (baseflow prior to event I; top), to intermediate flow conditions (peakflow during event I; middle), to the period of highest discharge for the studied events (peakflow during event III; bottom). Grey indicates the hydrologically disconnected areas (water level more than 30 cm from the soil surface), red indicates the hydrologically connected area (i.e., water level within 30 cm from the
625 **soil surface and connected to the stream via other active areas), and orange indicates the active but disconnected area (i.e., the water level increased into the upper 30 cm of the soil but is not connected to the stream by other active areas). The connected area was simulated based on the measured groundwater levels and a data-driven model that uses surface topography to estimate the water level for unmonitored grid cells, following the methodology of Rinderer et al. (2019).**

https://doi.org/10.5194/hess-2019-686
Preprint. Discussion started: 14 January 2020

Hydrology and Earth System Sciences
Discussions
Open Access
EGU

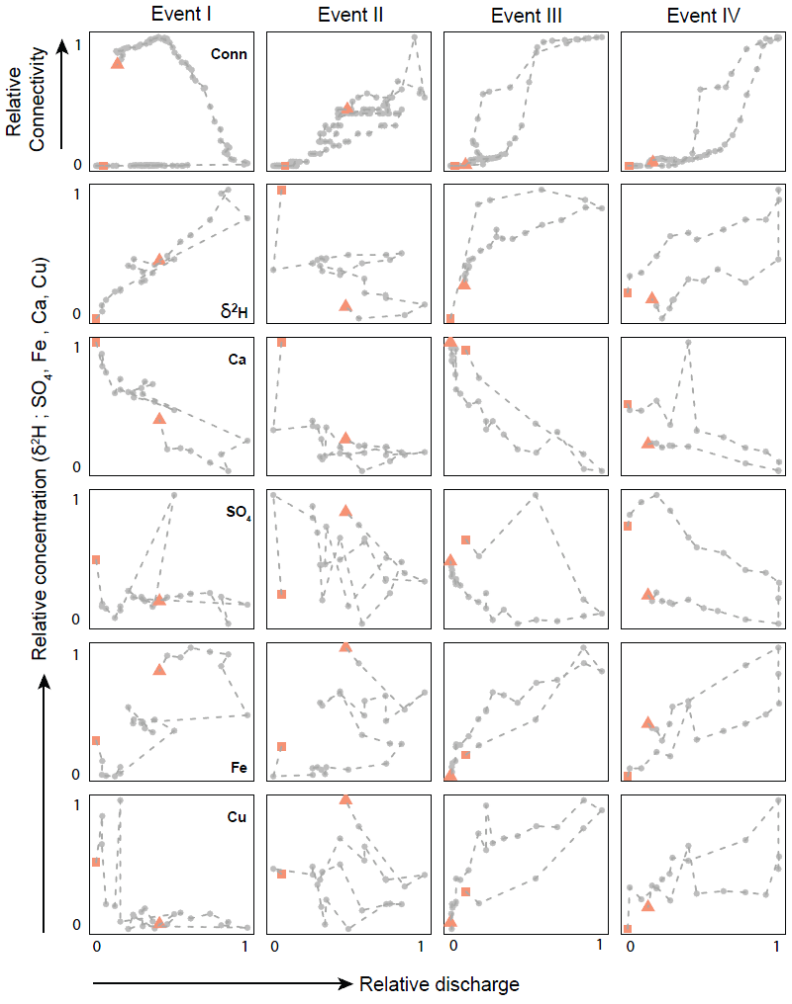

630 **Figure 5. Relation between the fraction of the catchment that was connected (Conn) and discharge (top row) and concentration-discharge relationships for δ^2H, calcium, sulfate, iron and copper (rows 2-6) from the start (orange square) until the end (orange triangle) of the event for events I-IV (columns). Individual samples are marked with a grey dot and connected with a dashed line. All data are normalized between 0 (minimum measured value for the event) and 1 (maximum measured value for the event) to better visualize the hysteretic relation.**

https://doi.org/10.5194/hess-2019-686
Preprint. Discussion started: 14 January 2020

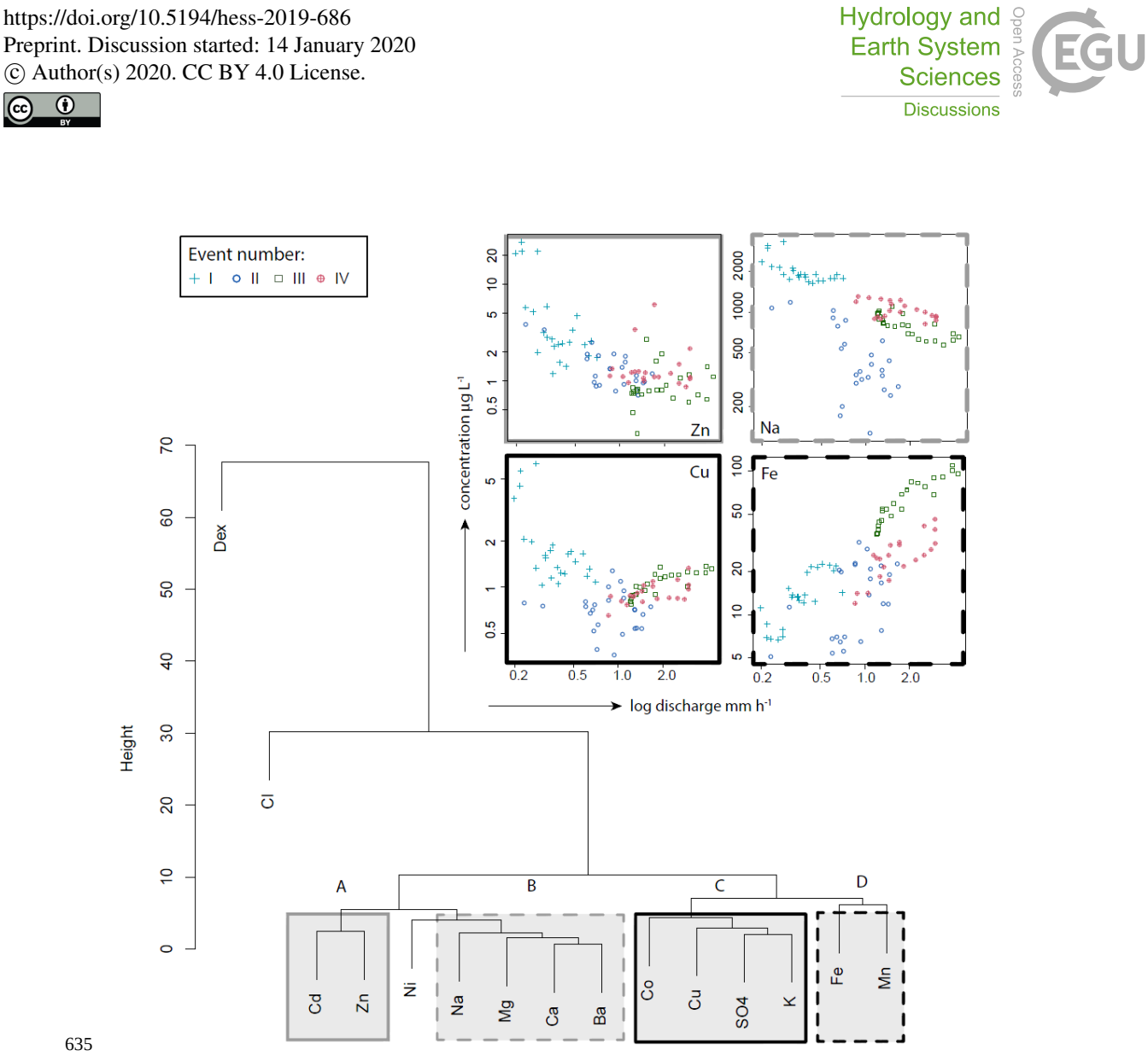

635

Figure 6. Bottom: Dendrogram for the hierarchical clustering of solutes and D_{ex} based on the magnitude and timing of changes in streamflow concentrations compared to the baseflow concentration (R_x; Eq. 2) during the four events, with different groups (A-D) marked in grey boxes, and top: concentration-discharge relationships for one solute from each of the four groups (different symbols indicate the different events).

https://doi.org/10.5194/hess-2019-686
Preprint. Discussion started: 14 January 2020

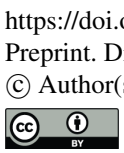

Hydrology and Earth System Sciences
Discussions
Open Access
EGU

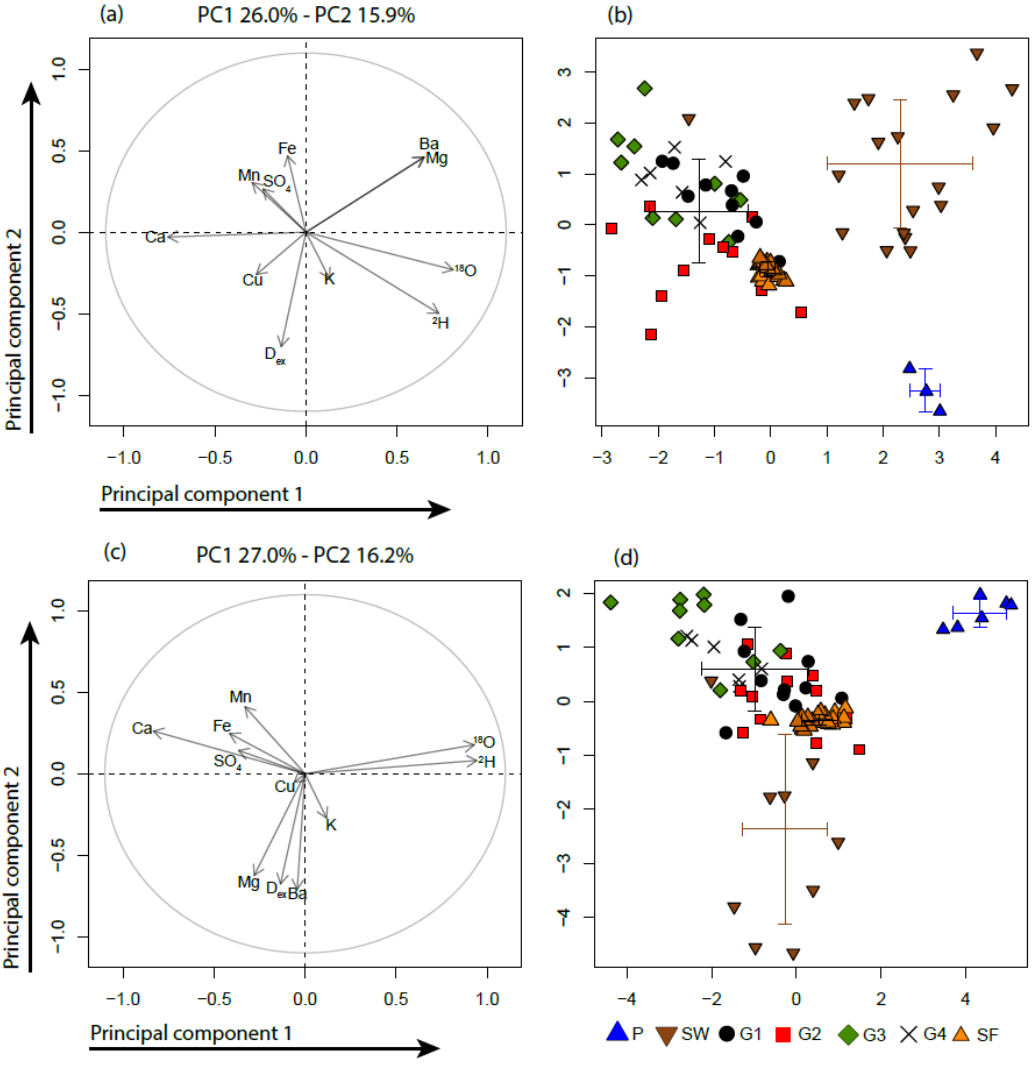

640

Figure 7. PCA results and mixing diagrams for event I (a and b) and event III (c and d). Event I is representative of a small event, whereas event III is representative of an intermediately sized event. In the biplots (a and c), the length of the arrow represents the explanatory power. The mixing diagrams based on the first two principle components (b and d) show the individual rainfall (blue triangles), soil water (brown reversed triangles), and groundwater samples (black circles, red squares, green diamonds and black
645 **crosses, representing groundwater types 1-4 based on Kiewiet et al., 2019), the streamflow samples (SF, orange triangles), as well as the average and standard deviation for each component (error bars). The biplots and mixing plots for the events II and IV are given in the supplementary material S3.**

https://doi.org/10.5194/hess-2019-686
Preprint. Discussion started: 14 January 2020

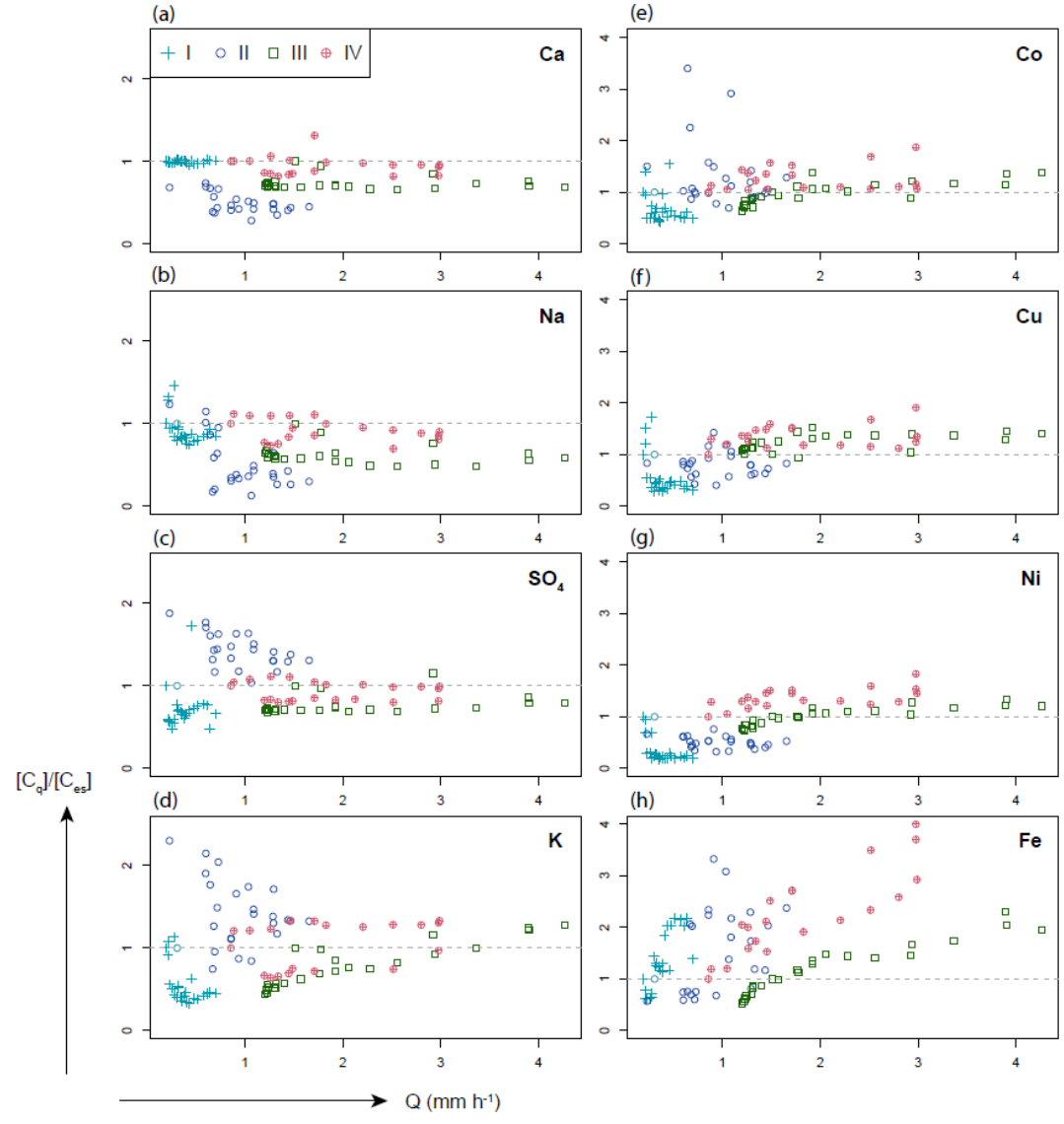

650 **Figure 8. The ratio of the measured (C_Q) and estimated stormflow concentrations (C_{es}; Eq. 3) for calcium, sodium, sulfate, potassium, cobalt, copper, nickel and iron as a function of the specific discharge (Q) at the catchment outlet. The dashed grey line indicates where C_Q and C_{es} are equal; the different symbols reflect the different events (I-IV). Note the difference in scale for the left and right column. For the relation with the fraction of the catchment that was connected to the stream see S4.**

https://doi.org/10.5194/hess-2019-686
Preprint. Discussion started: 14 January 2020

Hydrology and Earth System Sciences
Discussions
Open Access
EGU

Table 1. Overview of the four events analysed in this study: event duration (D, h), rainfall amount (P, mm), average and maximum 10-min rainfall intensity (I_p and $I_{p\text{-}max}$, mm h^{-1}), the range in specific discharge (ΔQ, mm h^{-1}), the maximum change in isotopic composition of the stream water (δ^2H, ‰), and the minimum and maximum fraction of the catchment that was connected (A_{min}-A_{max}) during the event, and the date of the groundwater and soil water sampling campaign.

Event	Start date	*D* [h]	*P* [mm]	I_p [mm h^{-1}]	$I_{p\text{-}max}$ [mm h^{-1}]	ΔQ [mm h^{-1}]	Q-δ^2H [‰]	A_{min}-A_{max} [-]	*Date of sampling campaign*
I	02 Oct 2016	14	17	1.2	7	0.02 – 0.07	-70.5 to -65.7	0.27 – 0.48	05 Oct. 2016
II	25 Oct 2016	28	33	1.2	13	0.02 – 0.17	-75.3 to -67.6	0.27 – 0.35*	05 Oct. 2016
III	03 Oct 2017	7	27	3.9	24	0.08 – 0.43	-73.7 to -69.1	0.33 – 0.68	12 Oct. 2017
IV	05 Oct 2017	27	32	1.2	10	0.07 – 0.30	-69.1 to -65.2	0.33 – 0.67	12 Oct. 2017

***The fraction of the catchment that was hydrologically connected increased from 0.27 to 0.28 during the sampling period, and to 0.35 during a discharge peak that occurred after the samplers stopped (see S2).**

Table 2. Average concentrations (± standard deviation) for all groundwater (GW_{avg}; n=335), all riparian groundwater (G1; n=99) and all hillslope groundwater (G2; n=99), soil water (SW; n=116), and rainfall samples (P; n=156). Solutes are ordered by their respective groups (section 4.3). Superscript letters $^{a\text{-}e}$ indicate the significantly different average concentrations.

Solute	Unit	GW_{avg}	G1	G2	SW	P
$\delta^{18}O$	‰	-11.0±0.9 ^{a}	-10.8±1.0 ^{ab}	-10.9±1.1 ^{ab}	-10.4±1.6 ^{b}	-12.3±4.0 ^{d}
$\delta^{2}H$	‰	-76.0±7.5 ^{a}	-74.3±8.0 ^{adb}	-74.9±9.1 ^{abd}	-70.8±12.4 ^{bd}	-84.4±33.0 ^{d}
D_{ex}	‰	12.0±0.8 ^{a}	12.4±0.8 ^{b}	11.8±0.9 ^{ab}	12.0±2.4 ^{ab}	14.1±3.2 ^{c}
Cl	µg L^{-1}	830.8±1076.5 ^{a}	708.8±570.1 ^{a}	890.5±804.9 ^{a}	1070.3±1026.6 ^{b}	327.1±348.7 ^{c}
Zn	µg L^{-1}	593.9±1745.7 ^{a}	720.4±2218.7 ^{a}	698.5±843.8 ^{b}	23.3±12.5 ^{b}	19.3±43.0 ^{c}
Cd	µg L^{-1}	0.05±0.08 ^{ad}	0.0±0.1 ^{ac}	0.1±0.1 ^{b}	0.03±0.06 ^{c}	0.1±0.2 ^{d}
Ni	µg L^{-1}	3.2±4.1 ^{a}	1.7±1.4 ^{b}	5.6±6.6 ^{c}	2.5±1.5 ^{a}	0.3±0.3 ^{d}
Na	µg L^{-1}	1587.6±2672.7 ^{a}	1107.1±1000.8 ^{ab}	827.6±341.3 ^{b}	839.1±565.0 ^{b}	148.7±153.5 ^{c}
Mg	µg L^{-1}	2235.7±1730.3 ^{a}	1292.5±684.3 ^{b}	1164.1±435.6 ^{b}	13612.8±10924 ^{c}	26.6±18.9 ^{d}
Ca	µg L^{-1}	56993.7±21966.1 ^{a}	44794.0±17097.6 ^{b}	55624.6±18099.0 ^{a}	22261.7±27287.8 ^{c}	213.4±202.7 ^{d}
Ba	µg L^{-1}	99.2±171.6 ^{a}	64.2±115.2 ^{b}	112.3±258.6 ^{a}	37350±27637 ^{c}	4.8±11.8 ^{d}
Co	µg L^{-1}	0.8±1.05 ^{a}	1.1±1.0 ^{a}	0.3±0.2 ^{b}	0.9±1.1 ^{a}	0.02±0.02 ^{c}
Cu	µg L^{-1}	64.9±143.7 ^{a}	7.4±16.1 ^{b}	175.5±211.8 ^{c}	5.2±9.0 ^{b}	1.4±1.0 ^{d}
SO_4	µg L^{-1}	3600.0±5112.5 ^{a}	2511.6±2843.2 ^{a}	2418.7±1848.2 ^{a}	1602.0±3061.9 ^{b}	623.1±980.1 ^{c}
K	µg L^{-1}	530.1±428.0 ^{a}	328.3±219.2 ^{b}	670.3±543.4 ^{a}	754.1±970.8 ^{a}	92.2±91.9 ^{d}
Fe	µg L^{-1}	390.7±1271.1 ^{a}	608.3±1648.4 ^{b}	25.4±38.6 ^{a}	254.3±775.9 ^{a}	3.5±7.1 ^{c}
Mn	µg L^{-1}	592.4±1111.6 ^{a}	1007.8±911.3 ^{b}	68.4±100.5 ^{c}	139.9±326.2 ^{c}	1.3±1.4 ^{e}

https://doi.org/10.5194/hess-2019-686
Preprint. Discussion started: 14 January 2020

Hydrology and Earth System Sciences
Discussions

Table 3. Summary of the groups of the presented solutes (A-D, based on the relative concentrations computed for all four events; Fig. 6; - indicates that this solute is not assigned to a group), the typical response of solute concentrations to increasing discharge (++: strong enrichment, mean R_x > 1.5; +: enrichment, mean R_x between 1 and 1.5; -: dilution, mean R_x < 1; ±: mixed response) and ratios between the average concentrations in soil water (C_{SW}) and groundwater (C_{GWavg}) and the groundwater from hillslope wells (C_{G2}) and riparian wells (C_{G1}) (see Table 2). See Fig. 5 and 6 for example concentration and discharge relations for each group of solutes. The solutes are sorted according to their typical response.

Solute	D_{ex}	Cl	Fe	Mn	Co	Cu	SO_4	K	Cd	Zn	Ni	Na	Mg	Ca	Ba
Group	-	-	D	D	C	C	C	C	A	A	-	B	B	B	B
Typical [C] response to increasing Q	++	++	+	+	±	±	±	±	±	±	±	-	-	-	-
Ratio C_{SW}/C_{GWavg}	1.0	1.3	0.7	0.2	1.1	0.1	0.4	1.4	0.6	~0	0.8	0.5	6.1	0.4	376.5
Ratio C_{G2l}/C_{G1}	1.0	1.3	~0	0.1	0.3	23.7	1.0	2.0	-	1.0	3.3	0.7	0.9	1.2	1.7

Table 4. Event-average fractions of groundwater (f_{GW}), soil water (f_{SW}), and rain water (f_P), based on the three-component End-Member Mixing Analyses, the pre-event water fraction (f_{pe}) based on the two-component hydrograph separation using δ^2H as a tracer, and the associated uncertainties for both calculations.

Event	Three-component End-Member Mixing Analyses				Two-component	
	f_{GW}	f_{SW}	f_P	uncertainty	f_{pe}	uncertainty
I	0.69	~0	0.31	0.93	0.91	0.16
II	0.21	0.33	0.45	0.60	0.76	0.31
III	0.39	0.38	0.22	1.59	0.78	0.35
IV	0.72	~0	0.28	1.43	0.97	0.19